*Science of Sintering,* **49** (2017) 431-443

doi: https://doi.org/10.2298/SOS1704431C

UDK: 622.785, 676.017.2

# Application of the Final Flotation Waste for Obtaining the Glass-ceramic Materials

**Mira Cocić[1*], Mihovil Logar[2], Suzana Erić[2], Viša Tasić[3], Snežana Dević[4], Saša Cocić[5], Branko Matović[6]**

[1]University of Belgrade, Technical Faculty in Bor, VJ 12, 19210 Bor, Serbia
[2]University of Belgrade, Faculty of Mining and Geology, Djusina 7, 11000 Belgrade, Serbia
[3]Mining and Metallurgy Institute Bor, Zeleni bulevar 35, 19210 Bor, Serbia
[4]Institute IMS Belgrade, Bulevar vojvode Misica 43, 11000 Belgrade, Serbia
[5]Reservoir Minerals Inc. TILVA D.O.O., Ustanicka 128a, 11000 Beograd, Serbia
[6]University of Belgrade, Vinča Institute of Nuclear Sciences, PO Box 522, 11000 Belgrade, Serbia

***Abstract:***

*This work describes the investigation of the final flotation waste (FFW), originating from the RTB Bor Company (Serbia), as the main component for the production of glass-ceramic materials. The glass-ceramics was synthesized by the sintering of FFW, mixtures of FFW with basalt (10%, 20%, and 40%), and mixtures of FFW with tuff (20% and 40%). The sintering was conducted at the different temperatures and with the different time duration in order to find the optimal composition and conditions for crystallization.The increase of temperature, from 1100 to 1480°C, and sintering time, from 4 to 6h resulted in a higher content of hematite crystal in the obtained glass-ceramic (up to 44%). The glass-ceramics sintered from pure FFW (1080°C/36h) has good mechanical properties, such as high propagation speed (4500 m/s) and hardness (10800 MPa), as well as very good thermal stability. The glass-ceramics obtained from mixtures shows weaker mechanical properties compared to that obtained from pure FFW. The mixtures of FFW with tuff have a significantly lower bulk density compared to other obtained glass-ceramics. Our results indicate that FFW can be applied as a basis for obtaining the construction materials.*

***Keywords****: FFW; Sintering; Glass-ceramics; Phase composition; Microstructure; Mechanical properties.*

## 1. Introduction

The extraction of copper, especially flotation enrichment and pyrometallurgical processing of the copper concentrates, generates waste materials [1]. Such waste material is a major source of environmental pollution. According to data obtained by RTB Bor Company, the total amount of smelting slag waste deposited at the landfill is about 16 million tons [2, 3]. In addition, a copper smelter in Bor (Serbia) every day produces additional 700-1000 tons of waste slag with an average copper content of about 0.75% [2, 3]. Furthermore, the mass of the flotation tailings, located near Bor town, is estimated at about 27 million tons, with an average

*) **Corresponding author:** mcocic@tf.bor.ac.rs

copper content of about 0.2-0.4% [2, 3].

These materials are with ferro-silicate composition, so that, the possibility of the utilization is of great importance, not only with the aim of reducing the industrial waste but also as a potential raw material for the new technologies.

The glass-ceramic materials obtained from the industrial wastes, rich in iron and glass were explored by many authors. Vitrification of a hazardous iron-rich waste from copper [4, 5] and zinc industry [6], provide chemically stable glass-ceramic materials with significantly better performance compared to traditional ceramic and natural building materials. The concrete which is the major material in the construction industry made with waste copper slag also affects the cost of construction comparable to pure concrete [7].

The blast furnace slags were used as additives to cementitious materials [8, 9] as well as to construction materials [9, 10]. The aluminosilicate glass with a low dielectric constant and dielectric losses [11] is obtained by mixing such slags with quartz sand. On the basis of glass from the Electric Arc Furnace Slag (EAFS) from 'Ezz Steel' in Egypt, the glass-ceramic material was obtained by heating at the temperature 850-870°C for 0.5 to 1h [12]. In addition, the glass-ceramic materials with excellent glaze characteristics were obtained by vitrification of the furnace slag from steel industry (BFS), thermal power plants ashes (FA), K- feldspar, and borax [13].

Basalt is an important raw material for the development of glass-ceramics as it is cheap, present in significant quantities, possess high chemical resistance, resistance to wear, and corrosion [14, 15]. The glass-ceramic materials with basalt and iron-rich glass similar basalt compositions have been developed for nuclear waste immobilization [16] and for vitrification industrial wastes which are environmental pollutants [3, 17-22]. The material of high crystallinity and good mechanical properties is obtained by sintering the pressed (100 MPa) alkali basalt tuff in the temperature range from 1000 to 1140°C [23]. By crystallization, the molten basaltic glass (basalt from the locality Vrelo Kopaonik, Serbia), at the temperature of 950°C over a period of 3h, the glass-ceramic material with dendritic structure was synthesized [14].

The application and use of zeolite tuffs for lightweight construction stone are known for centuries [24]. Especially, zeolite clinoptilolite $(Ca, Na, K)_{2\text{-}3}\ Al_3\ (Al, Si)_2\ Si_{13}\ O_{36} \bullet 12\ (H_2O)$, has been widely used in construction [24] as pozzolan in the cement production [25-27]. It was used as an additive to the composition of concrete mixtures [28, 29] to obtain lightweight concrete or as heat-insulating material [30].

The material obtained by melting the mixture of copper flotation slag (30%), blast furnace slag (30%) and zeolitic tuff (40%), has a high degree of crystallization, suitable for the production of glass-ceramic [4].

This paper describes the research of potential application of FFW for obtaining the glass-ceramic materials.The glass-ceramics was synthesized by sintering the FFW (RTB Bor, Serbia), and FFW mixture with basalt (Slavujevac near Presevo, Serbia) and with tuff (Igros near Brus, Serbia). In order to find the optimal composition and conditions for the crystallization, the sintering was done at the different temperatures and with the different time duration. The other aims of our research were to correct the dynamics of liquid phase development, to lower the sintering temperature, sintering interval, and density.

## 2. Experimental

### 2.1. Material and methods

To complete valorization of copper, copper smelter slag is further processed in the flotation plant. At the beginning, the slag is chopped (grain size below 12 mm) and then ground, first in the mill with rods (up to 2-3mm), then in the ball mill (60% of the grains finer than 74μm). The product of grinding is subjected to the flotation. As a product of the flotation

process, copper concentrate is extracted in the form of pulp. Waste material from the flotation process is transported to the thickeners and after thickening deposited in the flotation tailings.

The FFW was sampled at the flotation output prior to transport to the landfill. To examine the applicability of FFW the appropriate tests were carried out that can be divided into two groups. The first group of tests included the characterization of starting materials (FFW, basalt, and tuff). This means the examination of phase composition and thermal properties (interval of sintering, softening and melting). The second group of tests included obtaining and characterization the obtained glass-ceramics.

The sintering temperature was projected based on the thermal properties of starting materials and the data from the following references [4, 5, 23, 31-33].

The glass-ceramic materials were synthesized by sintering the samples in the presence of a liquid phase. The FFW sintering interval is difficult to control, so the addition of filler is necessary. The physical properties of filler (tuff or basalt) should serve to improve the properties of the final product whilst FFW should provide a liquid phase for sintering.

The phase composition was determined by X-ray powder diffraction (XRPD). The diffraction patterns were obtained using a Siemens D500 diffractometer. The phases ratio has been determined by the Powder Cell (PCW) software using structural models of magnetite [34], fayalite, hematite, and maghemite [35-37].

The chemical composition of FFW is determined by X-ray fluorescence analysis (XRF PANalytical Axios Spectrometer). The microstructure of the synthesized glass-ceramic has been tested on JEOL JSM-6610LV Scanning Electron Microscope (SEM). Samples were covered with carbon using BALTEC-SCD-005 Sputter coating device and recorded under conditions of high vacuum. LaB6 filament was used as a source of electrons. Chemical analyzes of all samples were performed on energy-dispersive spectrometer type X-Max Large Area Analytical Silicon Drift (Oxford). All samples were vaporized with carbon at BALTEC-SCD-005 vaporizer. The thickness of carbon layer was 18 nm. The optical microscopy observation was done on the LEITZ-ORHTOPLAN Wetzlar microscope (missed light) (OM).

To test the thermal properties of the FFW, powder sample is dry pressed under a pressure of 60 MPa in a mold (cube 4x4x4 mm). Intervals of sintering, softening and melting of the cube samples were determined by thermomicroscope Carl Zeiss - Jena equipped with video system and digital camera (Canon PRO-1) for the automatic recording and monitoring. The changes of the sample were monitored and recorded in the temperature range between 20 and 1500°C.

The characteristics of the synthesized glass-ceramic bodies obtained from FFW, T20 and T40 (1080°C/36h), and from P20, and P40 (1000°C/48h) were evaluated by measuring the bulk density, hardness, propagation speed of the longitudinal ultrasound waves and the resistance to thermal shock (successively raising the temperature up to 800°C). The changes in hardness and propagation speed were monitored before and after the thermal shocks. The hardness is determined using a Vickers durometer Meopta PRAHA. The propagation speed was measured by the Krautkramer-UDP-1 (Iskra), using the probes: MB 4 S - N and B 2S-N.

## 3. Results and Discussion

### 3.1. Characterization of the starting materials

The chemical and phase composition of the starting materials (FFW, basalt, and tuff) is shown in Tab. I. The most present components in the chemical composition of FFW are iron oxides and silicon while in basalt and tuff are oxides of silicon and aluminum.

According to X-ray powder diffraction analysis, the major mineral phases of FFW are magnetite and fayalite, basalt consists of albite, diopside, K-feldspar, and leucite while tuff consists of clinoptilolite, plagioclase, biotite, and smectite [3]. The phase composition of FFW

(Tab. I) is calculated based on the XRPD using Rietveld analysis and chemical composition, using the theoretical, stoichiometric formulas for fayalite and magnetite. FFW consists of fayalite (40%), magnetite (25% ) and glass (35%).

**Tab. I** Chemical and phase composition of starting material.

| Oxides | Share (%) | | | | | |
|---|---|---|---|---|---|---|
| | FFW | | | | Basalt | Tuff |
| | | *Mt* | *Fy* | *Glass* | | |
| $SiO_2$ | 34.27 | - | 13.64 | 20.63 | 54.35 | 57.91 |
| $TiO_2$ | 0.36 | - | - | 0.36 | 1.08 | 0.54 |
| $Al_2O_3$ | 4.89 | - | - | 4.89 | 15.86 | 11.44 |
| $Fe_2O_3$ | 52.10 | 25.34 | 25.97 | 0.78 | | |
| FeO | | - | - | | 6.44 | 4.54 |
| $Mn_3O_4$ | 0.07 | - | - | 0.07 | | |
| MgO | 0.79 | - | - | - | 6.19 | 1.47 |
| CaO | 4.58 | - | 0.79 | 4.58 | 7.86 | 5.11 |
| $Na_2O$ | 0.31 | - | - | 0.31 | 3.7 | 0.95 |
| $K_2O$ | 1.2 | - | - | 1.22 | 3.84 | 0.72 |
| $P_2O_5$ | 0.07 | - | - | 0.07 | | |
| $SO_3$ | 0.5 | - | - | 0.5 | | |
| CuO | 0.49 | - | - | 0.49 | | |
| ZnO | 0.79 | | - | 0.79 | | |
| $H_2O^+$ | | | | | | 14.43 |
| $H_2O^-$ | | | | | | 3.6 |
| sum % | **100.44** | 25.34 | 40.4 | 34.7 | **99.32** | **100.71** |
| Phase composition | Fy, Mt, glass | | | | Ab, Dy, Kf, Lc | Kp, Pl, By, Sm |

**Legend:** FFW - Final flotation waste, Fy - fayalite ($Fe_2SiO_4$), Mt - magnetite ($FeFe_2O_4$), Ab - albite ($NaAlSi_3O_8$), Dy - diopside ($CaMgSi_2O_6$), Kf - K feldspate, Lc - leucite, Kp - clinoptilolite $(Ca,Na,K)_{2\text{-}3}\ Al_3(Al,Si)_2\ Si_{13}\ O_{36}\ x\ n(H_2O)$, Pl - plagioclase, By - biotite $(K(Mg,Fe)_3AlSi_3O_{10}(OH,F)_2)$, Sm – smectite.

Thermal characteristics of starting materials are shown in Tab. II and in Fig. 1 (temperature changes 12 °C/min). The lowest start and end of sintering temperatures are observed for FFW. The sintering interval of basalt is narrow (1068 - 1120°C) in comparison with FFW.

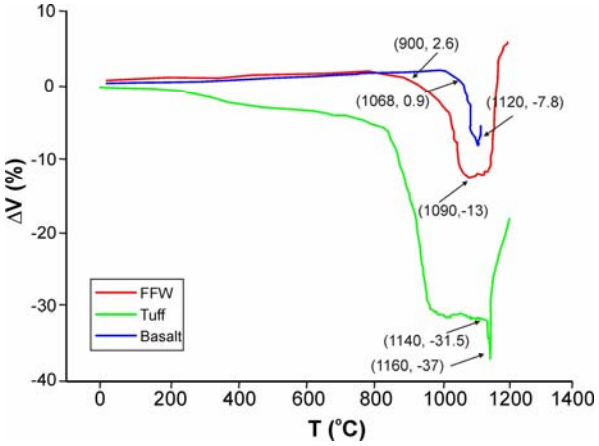


**Fig. 1.** Changes in volume of starting materials as a function of temperature.

Clinoptilolite is the dominant mineral in tuff. The dehydration of clinoptilolite causes shrinkage (2%) in the temperature range from 240 to 350°C. The collapse of the clinoptilolite

structure causes great contractions in the temperature range from 850 to 950°C. The development of liquid phase started at 1140°C (start of sintering). The end of sintering occurs at 1160°C, with the test body deformation. The sintering interval of tuff is the narrowest in comparison with the other starting materials as well the change of volume.

### 3.2. Synthesis of glass-ceramics from the glass frit of FFW

In order to obtain a frit, the sample of FFW is thermally treated at 1300°C, for 2-4h, then rapidly cooled in water, and pulverized in the vibrating mill. Thereafter samples were sintered at 1100 °C/4h, 1150 °C/4h, and 1480 °C/6h.

Sintering the frit of FFW at a temperature of 1100°C, for 4h, resulted in glass-ceramics with bubble structure (Fig. 2). This is due to the emanation of gases caused by thermal treatment. Such structure has good insulating properties.

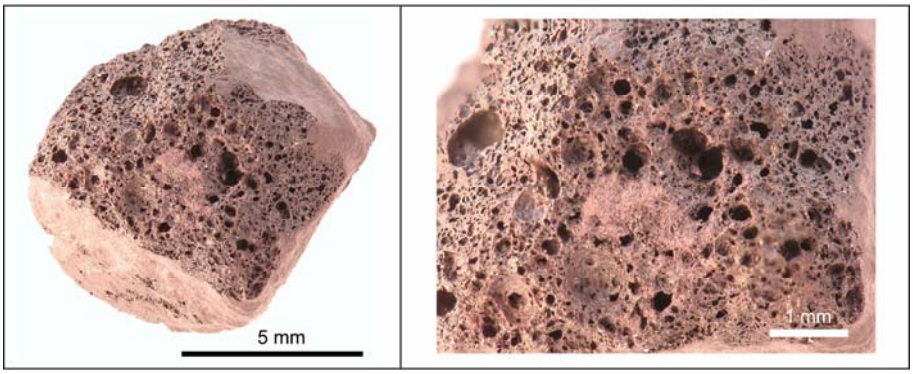


**Fig. 2.** Macro photographs of the glass-ceramic samples obtained from the glass frit of FFW at 1100°C/4h.

Diffraction patterns of synthesized glass-ceramics (1100 °C/4h, 1150 °C/4h, and 1480 °C/6h) are shown in Fig. 3. Because of the intensive oxidation, magnetite is transformed into the hematite [9, 38] while fayalite is transformed into the hematite and amorphous glass [9, 39].

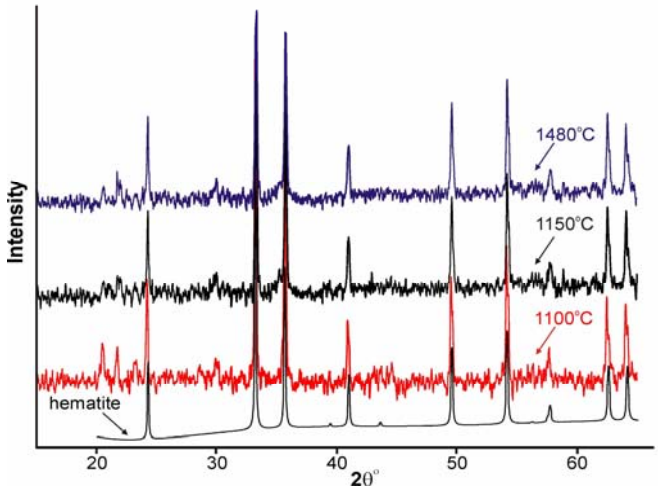


**Fig. 3.** X-ray powder diffraction diagrams of glass-ceramics obtained from the glass frit of FFW at 1100 °C/4h, 1150 °C/4h, and 1480 °C/6h.

The microstructure of synthesized glass-ceramic consists of the glass and crystals of hematite. The glass-ceramic obtained at 1100 °C/4h and 1150 °C/4h (Fig. 4) consists of solid solution where two phases are observed: hematite and magnetite. The crystals are anhedral, rarely subhedral, with a diameter generally below 10 μm. At 1480 °C/6h (Fig. 4) the viscosity drops and the glass spills.When the glass is at the point of spillage it causes oxidation of $Fe^{2+}$ to $Fe^{3+}$ [17, 40-42], resulting in changes in the chemical composition of surface and subsurface layers. At that moment, the surface is to the greatest extent exposed to oxidation, and hematite development culminating in a large number of euhedral crystal whose content reaches 44%.

The average content of crystal phases of synthesized glass-ceramic is determined by digital image analysis of at least 10 digital images per each temperature of interest (Fig. 4). The content of the hematite at 1100 °C/4h is 26.7%, at 1150 °C/4h is32 %, while at 1480 °C/6h is 44%. By changing the conditions of heat treatment and cooling modes microstructure and properties of products can be controlled and desirable glass-ceramic materials can be produced [4, 5].

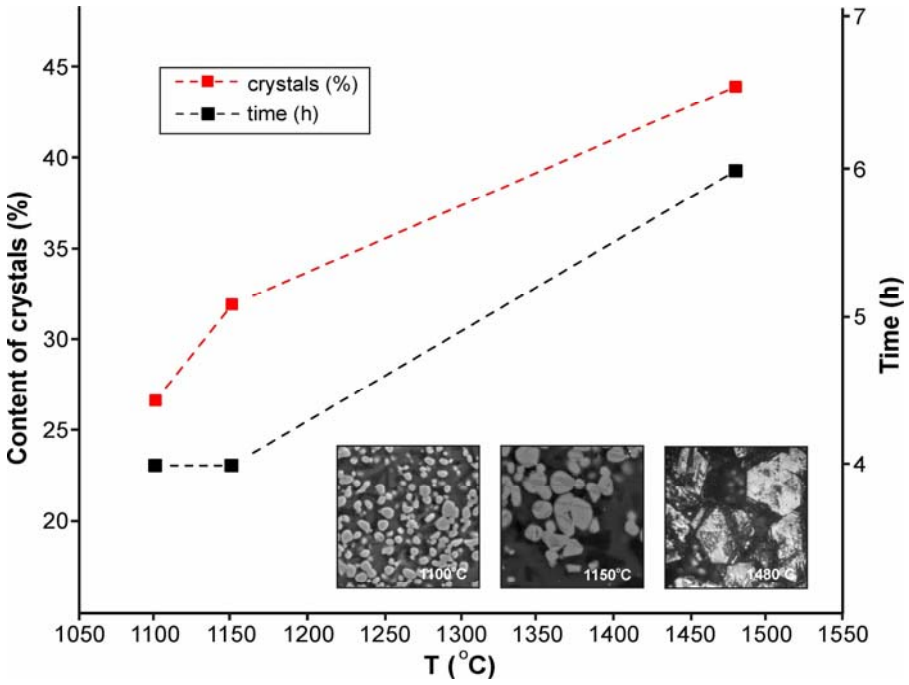


**Fig. 4.** The average content of crystals in the glass-ceramics sintered from the glass frit of FFW with examples of the analyzed digital images.

## 3.3. Synthesis of glass-ceramic from mixtures: P10, P20, P40, T20, and T40 at 1260 °C/7h

To obtain glass-ceramics with the improved properties in comparison with those obtained from FFW, the mixtures of FFW with basalt (P10, P20, and P40) and tuff (T20 and T40) were heated at a temperature of 1260°C for 7h. Such obtained glass-ceramics consists of a vitreous phase and the iron-oxide crystals (as shown in Fig. 5). In some crystals, the zone separation is observed which indicates a difference in Fe distribution between the dark and the light gray zone. Such morphology is a typical for the hematite crystals, due to subhedral rhombohedral crystals. In addition to chemical variations, structural variations are also

observed. The hematite, magnetite, and maghemite are identified by X-ray powder diffraction as shown in Fig. 6.

In glass-ceramics obtained from P10 (Fig. 5a), iron-oxide crystals appear in small, anhedral, rarely subhedral forms. Also, such crystals can be observed in the form of small rounded crystals, connected into dendrites [43].

In glass-ceramics obtained from P20 (Fig. 5b) and P40 (Fig. 5c), individual iron oxide crystal appears in the subhedral and euhedral rhombohedral form. Dendritic aggregates, however, are very widespread.

In glass-ceramics obtained from T20, the iron-oxide crystals (Fig. 5d) appear in the form of dendritic aggregates. Such microstructure of glass was also reported by M. Romero and J. Ma. Rincon [44]. In glass-ceramics obtained from T40, the iron-oxide crystals (Fig. 5e) form dendrites which are concentrated in one part of the sample while in another part of the sample they appear as individual crystals.

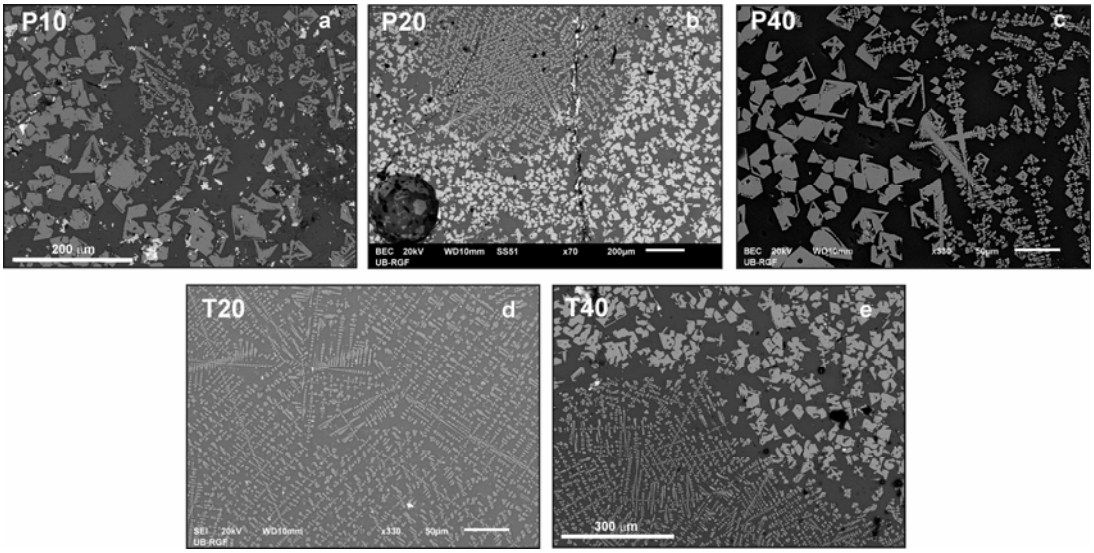


**Fig. 5.** Microphotography (SEM) of the glass-ceramics obtained from: a) P10, b) P20, c) P40, d) T20, and e) T40.

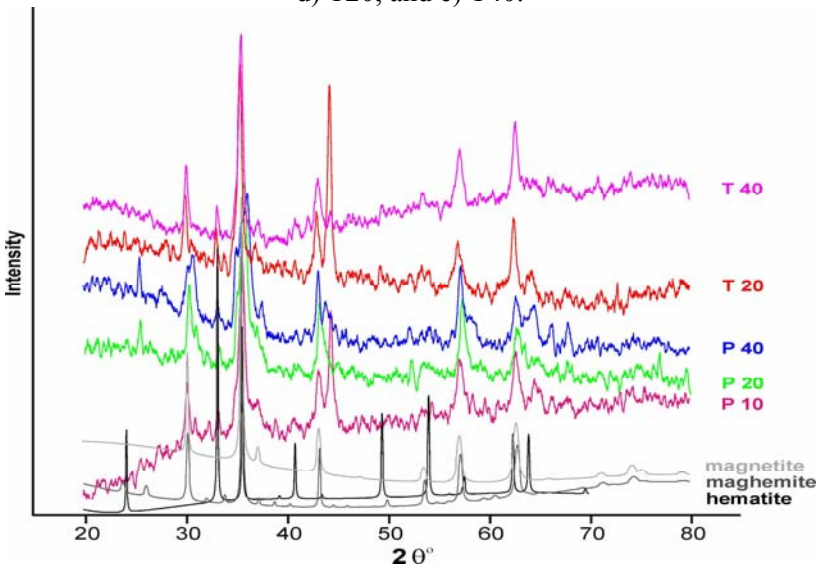


**Fig. 6.** X-ray powder diffraction diagrams of the obtained glass-ceramics.

The changes in dimensions of the samples caused by heating are given in Tab. II and shown in Fig. 7. The heating mode is the same as for the starting material samples (12 °C/min).

**Tab. II** Thermal characteristics of starting materials and mixtures.

| Thermal characteristics | Samples | | | | | | | |
|---|---|---|---|---|---|---|---|---|
| | Starting materials | | | FFW mixtures with basalt | | | FFW mixtures with tuff | |
| | FFW | Basalt | Tuff | P10 | P20 | P40 | T20 | T40 |
| Start of sintering (°C) | 900 | 1068 | 1140 | 1095 | 1095 | 1090<br>1118 | 1080 | 1080 |
| End of sintering (°C) | 1090 | 1120 | 1160 | 1120 | 1120 | 1120 | 1160 | 1160 |
| Interval of sintering (°C) | 190 | 52 | 20 | 25 | 25 | 30<br>2 | 80 | 80 |
| Change in volume (%) | 13 | 7.8 | 5.5 | 13 | 13 | 10 | 7 | 7 |

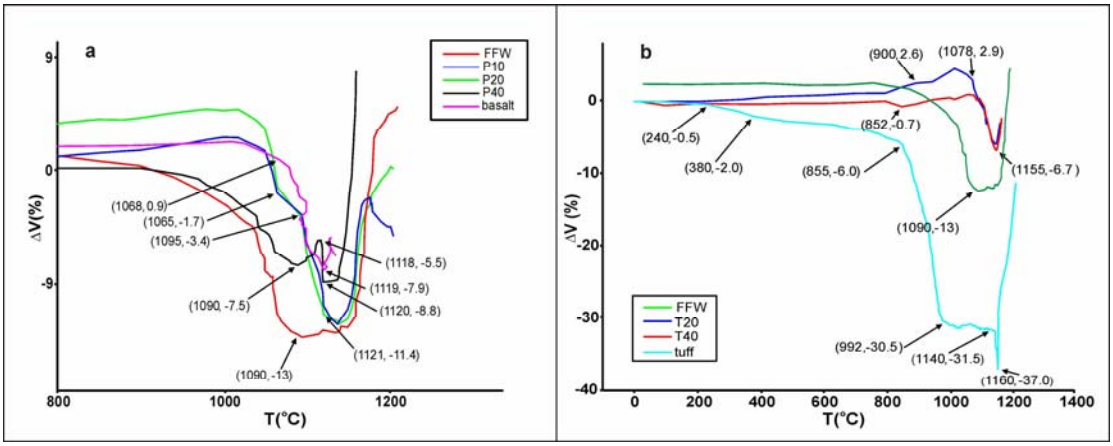


**Fig. 7.** Changes in the volumes of starting materials and mixtures as a function of temperature:
a) FFW, basalt, P10, P20 and P40, b) FFW, tuff, T20, and T40.

Basalt and tuff have higher temperatures of start and end of sintering, but less volume changes and narrower sintering interval, compared to FFW.

The sintering of two mutually separated systems is observed in P40, defined by volume minimums at 1090°C (7.4%), and 1120°C (8.8%). Their volume minimums coincide with the end of sintering temperatures of pure FFW and basalt. The contraction of components is proportional to their participation in the mixture. The observed difference of 2% (1090°C to 1118°C) between the theoretical and measured contraction is caused by dilatation, due to the limited penetration of the liquid phase of FFW in the pore space of basalt particles. The sintering of basaltic particles starts with the development of the liquid phase at 1118°C and the sintering process ends very fast at the 1120°C.

In P10 and P20 mixtures, the fall of contraction kinetics in the temperature range from 1065°C to 1095°C is observed. Because of the relatively low concentrations of basalt (10-20%), the pore space is mainly from FFW particles. Therefore the total amount of shrinkage is similar to that of pure FFW. The reaction between fluid phases of two components moves the end of sintering to a higher temperature.

Mixtures T20 and T40 do not exhibit contraction caused by the collapse of the structure of clinoptilolite in the temperature range from 850°C to 900°C that occurs in pure tuff. The effect is absent because the temperature interval coincides with the development of liquid phase of FFW. The reaction of FFW liquid phases with clinoptilolite does not allow a structural collapse. The start of sintering for both mixtures occurs at the end of the sintering temperature of FFW (1080°C). The end of sintering temperatures for both the mixtures coincides with the end of the sintering temperature of pure tuff (1160°C).

### 3.4. Synthesis of glass-ceramics from FFW, T20, T40, P20 and P40

The lozenges were made from each sample (FFW, P 20, P 40, T20, and T40) by putting the 35g of sample into the cylindrical mold (3 cm in diameter) that are pressed at a pressure of 70 MPa. Such prepared samples were sintered in an electric furnace at a temperature of 1080°C for 36h. Synthesized glass-ceramic is shown in Fig. 9. Samples P20 and P40 exhibit a complete deformation so they have been sintered again. In order to avoid excessive development of the liquid phase that samples were sintered at the temperature of 1000°C for 48 h (Fig. 8).

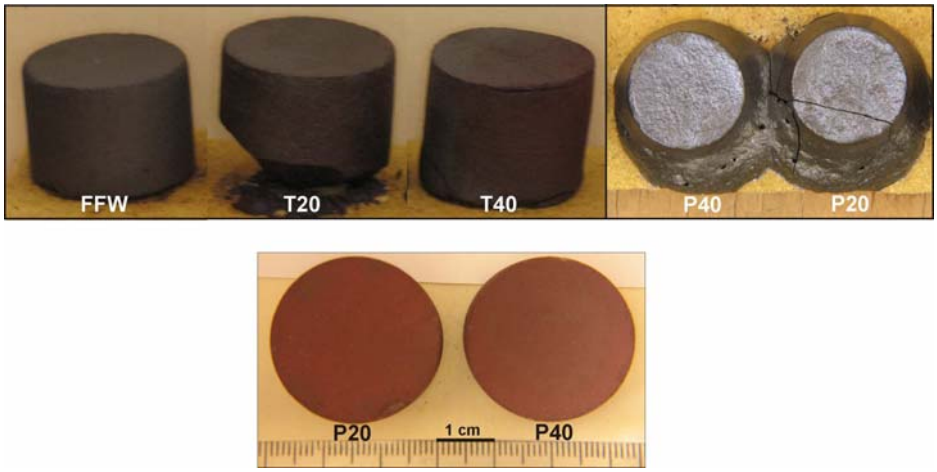


**Fig. 8.** Samples sintered at: 1080 °C/36h (above), and 1000 °C/48h (below).

Characteristics of the sintered glass-ceramic bodies were evaluated by measuring: bulk density, Vickers hardness, propagation speed of the longitudinal ultrasound waves and exposure to thermal shocks (samples were heated to 110 °C/1h, 200 °C/1h, 400 °C/1h and 800 °C/1h, and then cooled in water at temperature from 15°C to 20°C). The changes in hardness and propagation speed were measured during the thermal shock tests.

The densities of the sintered samples of FFW, P20, P40, T20, and T40 were 3.06, 2.9, 3.1, 2.4 and 2.5 respectively.

By observing the propagation speed the sintered samples can be classified into two groups (Fig. 9a). The first group consisted of samples: FFW (4500 m/s), T20 (4150 m/s), and T40 (4100 m/s). By observing the FFW sample, the propagation speed decreases slowly up to a temperature of 400°C. Above this temperature, the rapid decline of propagation speed is observed. By contrast, observing the T40 and T20 samples, the propagation speed decreases at temperatures of 200°C, and at 100°C, respectively, after which decreases linearly up to the temperature of 800°C (Fig. 9a).

The second group of samples consists of P20 (2080 m/s) and P40 (2230 m/s) (Fig. 9a). Concerning the P20 sample, almost constant propagation speed is observed up to thermal shock at 400°C. By contrast, the P40 sample propagation speed suddenly drops after

200°C. For this group, the measurement of the propagation speed was impossible after the thermal shock at 400°C due to a permeability drop (dotted line in the Fig. 9a). This indicates the presence of a discontinuity that disseminates ultrasound waves. This samples becoming impermeable for ultrasound waves, indicating that FFW significantly better reacts during the sintering with the tuff particles, compared to basalt.

The measurement of Vickers hardness supports a finding that the glass-ceramics sintered from FFW are a very hard material. The hardness of the sintered glass-ceramics is 10800 MPa, whilst the hardness of glass is 5000 – 10000 MPa (http://www.dynacer.com/properties/hardness). The hematite crystals, occurring in the sintering process, certainly contribute to such high values of the hardness of the sintered glass-ceramics. The hardness of sintered glass-ceramics rapidly decreases (from 10800 to 1730 MPa) under the thermal shocks. Other samples showed much lower hardness (Fig. 9b) with negligible changes in hardness under the thermal shocks.

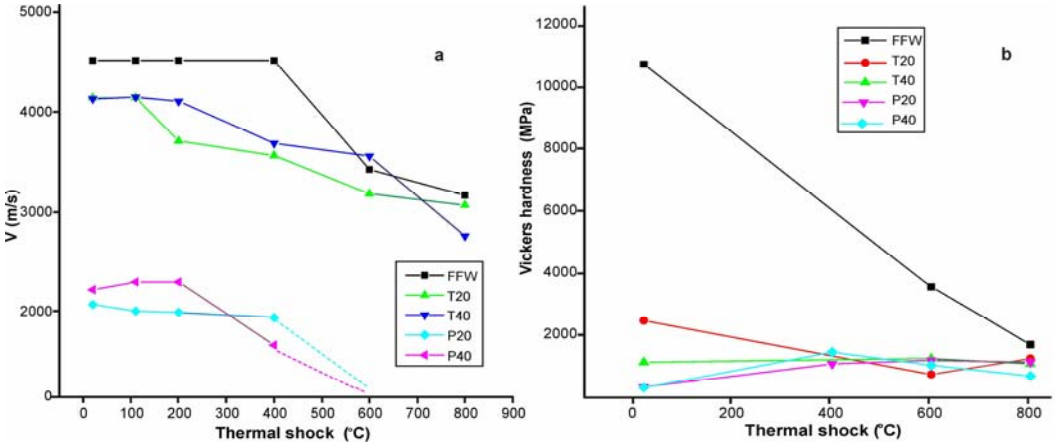


**Fig. 9.** a) The propagation speed of longitudinal ultrasound waves as a function of thermal shock temperature, b) Measured Vicker's hardness as a function of thermal shock temperature.

The glass-ceramics sintered from the mixtures express smaller changes under the thermal shocks compared with the glass-ceramics sintered from FFW. It also testifies to the different strengths of the connection between the sintered particles in samples with the different composition. The bond strength between the sintered particles predominantly depends on the composition of the liquid phase. The FFW has a hardness that is much higher than of sintered tiles (4240 MPa) [3] and retains its property up to the thermal shock of 600°C (Fig. 10b). Therefore, the glass-ceramics sintered from FFW could be used in the construction industry where thermal stability at 200°C or 400°C is required. The mixtures of FFW with tuff and basalt would also find the application in this fields, particularly in areas where good sound insulation is required.

## 4. Conclusions

In this work, the investigation of FFW, originating from the RTB Bor Company (Serbia), as the main component for the production of new glass-ceramic materials is described. It was confirmed that FFW consists of fayalite (40.4%), magnetite (25.3%) and glass (34.7%). The glass-ceramics was synthesized by the sintering of pure FFW, from a mixture of FFW with basalt (10%, 20%, and 40%) and tuff (20%, and 40%). The sintering

was done at the different temperatures and with the different time duration in order to find the optimal composition and conditions for the crystallization.

The glass-ceramic material obtained by sintering the pressed glass frit of FFW at a temperature of 1100°C, and 1150°C, for 4h, has bubble structure and consists of a vitreous phase and hematite crystals. Sintering the pressed glass frit of FFW at 1480°C for 6h resulting in glass-ceramics rich of large rhombohedral crystals of hematite (44%). With the increase of temperature and time of sintering, a higher content of crystals is obtained. It confirmed that by changing the conditions of heat treatment and cooling modes microstructure and properties of products can be controlled and desirable glass-ceramic materials can be produced.

The glass-ceramic material obtained by sintering the mixture of FFW and basalt or FFW and tuff at a temperature of 1260 °C/7h, consists of a vitreous phase and the iron-oxide crystals, which are often euhedral, and appears in the form of dendrites. The iron-oxide crystals are maghemite, magnetite, and hematite.

The glass-ceramic material obtained by sintering the compacted samples of FFW at 1080 °C/36h, has excellent mechanical properties (high propagation speed (4500 m/s) and, Vickers hardness (10800 MPa) and very good thermal stability. The glass-ceramic materials obtained by sintering the compacted samples of mixtures (T20, and T40 at 1080 °C/36h, P20, and P40 at 1000 °C/48h) have worse mechanical properties compared with the glass-ceramics sintered from pure FFW. FFW reacts better with tuff particles than with particles of basalt. The relatively low-shrinkage of mixtures of FFW with tuff (about 7%) enables reliable shape control of the final products. Test results indicate that FFW can be applied as a basis for obtaining the construction materials.

A very good resistance to thermal shocks shows that it can be also applied in other industrial areas, that requires additional tests. By adding alkali-rich materials the melting point lowers so that further tests should be also continued in that direction.

## Acknowledgements

This work was partly funded by the Grant of the Ministry of Education, Science and Technological Development of the Republic of Serbia, project 176010: “Composition, genesis, application, and contribution to the environmental sustainability”.

## 5. Refrences

1. M. Dimitrijevic, A. Kostov, V. Tasic and N. Milosevic, J. Hazard. Mater. 164, 892 (2009).
2. R. Stanojlović, Z. Stirbanovic and J. Sokolovic, J. Min. Metall. Sect. A: 44, 44 (2008).
3. M. Cocic, Application of the flotation waste from the RTB Bor for glass – ceramics. Ph.D. thesis, University of Belgrade, Faculty of Mining and Geology, Belgrade, Serbia (2012).
4. Karamanov, M. Aloisi and M. Pelino, J. Hazard. Mater. 140, 333 (2007).
5. S. Coruh, O. Nuri Ergun and T. Cheng, Waste Manage. Res. 24, 234 (2006).
6. M. Pelino, Waste Manage. 20, 561 (2000).
7. K. Murari, R. Siddique and K. K. Jain, J. Mater. Cycles. Waste Manag. 17, 13 (2015).
8. Alp, H. Deveci, and H. Sungun, J. Hazard. Mater. 159, 390 (2008).
9. B. Gorai, R. K. Jana, and Premchand, Resour. Conserv. Recy. 39, 299 (2003).
10. P. Asokana, M. Saxena, and S.R. Asolekar, Build. Environ. 42, 2311 (2007).

11. S. Li, S. Huang, H. Liu, F. Wu, Z. Chang and Y. Yue, JOM, 67, 2754 (2015).
12. Kamusheva, E. M. A. Hamzawy and A. Karamanov, Journal of Chemical Technology and Metallurgy 50, 512 (2015).
13. H. Lu, M. He, Y. Liu, J. Guo, L. Zhang, D. Chen, H. Wang, H. Xu and R. Zhang, J. Ceram. Process. Res. 12, 588 (2011).
14. M. Cocic, M. Logar, B.Matović and V. Poharc-Logar, Sci. Sinter. 42, 383 (2010).
15. B. Matović, S. Bošković and M. Logar, J. Serb. Chem. Soc. 68, 505 (2003).
16. M. I. Ojovan, J. M. Juoi1 and W. E. Lee, J. Pak. Mater. Soc. 2, 72 (2008).
17. Karamanov, P. Pisciella, C. Cantalini and M. Pelino, J. Am. Ceram. Soc. 81, 3153 (2000).
18. G. Scarinci, G. Brusatin, L. Barbieri, A. Corradi, I. Lancellotti, P. Colombo, S. Hreglich and R. Dalligna, J. Eur. Ceram. Soc. 20, 2485 (2000).
19. Karamanov and M. Pelino, J. Non-Cryst. Solids. 281, 139 (2001).
20. P. Kavouras, P. Komninou and K. Chrissafis, J. Eur. Ceram. Soc. 23, 1305 (2003).
21. P. M. Surensen, M. Pind, Y. Z. Yue, R. D. Rawlings, A. R. Boccaccini and E. R. Nielsen, J. Non-Cryst. Solids. 351, 1246 (2005).
22. P. Kavouras, T. Kehagias, I. Tsilika, G. Kaimakamis, K. Chrissafis, S. Kokkou, D. Papadopoulos, and Th. Karakostas, J. Hazard. Mater. A 139, 424 (2007).
23. Karamanov. L. Arrizza, and S. Ergul, J. Eur. Ceram. Soc. 29, 595 (2009).
24. Margeta, A. Farkaš and Z. Glasnović, Građevinar 63, 1009 (2011).
25. Ahmadi and M. Shekarchi, Cement Concrete Comp. 32, 134 (2010).
26. Bilim, Constr. Build. Mater. 25, 3175 (2011).
27. V. Sasnauskas, G. Rinkevičius, D. Martinavičius, D. Vaičiukynienė and E. Ivanauskas, JSACE 2, 11 (2015).
28. A. Ramezanianpour, A. Kazemian, M. Sarvari and B. Ahmadi, J. Mater. Civ. Eng. 25, 589 (2013).
29. Karakurt, H. Kurama, and I. Bekir Topçu, Cement Concrete Comp. 32, 1 (2010).
30. S. Djambazov, A. Yoleva, P. Chervenliev and A. Georgiev, Journal of Chemical Technology and Metallurgy 50, 520 (2015).
31. Karamanov, G. Taglieri and M. Pelino, J. Am. Ceram. Soc. 82, 3012 (1999).
32. M. Rincon, J. Càceres, C. J. Gonzàles-Oliver, D. O. Russo, A. Petkova and H. Hristov, J. Therm. Anal. Calorim. 56, 931 (1999).
33. Karamanova, S. Ergul, M. Akyildiz and M. Pelino, J Non-Cryst. Solids. 354, 290 (2008).
34. E. Fleet, Acta Crystallogr. B 37, 917 (1981).
35. J. R. Smyth, Am. Mineral. 60, 1092 (1975).
36. E. N. Maslen, V. A. Streltsov, N. R. Streltsova and N. Ishizawa, ASBSD 50, 435 (1994).
37. Greaves, J. Solid State Chem. 49, 325 (1983).
38. H. St. C. O'Neill, Am. Mineral. 73, 470 (1988).
39. S. J. Mackwell, Phys Chem. Minerals. 19, 220 (1992).
40. R. D. Cooper, J. B. Fanselow, and D. B. Poker, Geochim. Cosmochim. Acta 60, 3253 (1996).
41. J. M. Burkhard, and T. Scherer, J. Non-Cryst. Solids 352, 241 (2006).
42. Schreiber, B. K. Kochanowski, and C. W. Shreberg, J. Am. Ceram. Soc. 39, 141 (1994).
43. Badillo, D. Ceynar, and C. Beckermann, J. Cryst. Growth 309, 197 (2007).
44. Romero and J. Ma. Rincon, J. Eur. Ceram. Soc. 18, 153 (1998).

***Садржај***: *У раду је испитана могућност примене дефинитвне флотацијске јаловине пореклом из компаније РТБ Бор (Србија) за производњу нових материјала из групе стаклокерамике. Синтетисана је стаклокерамика синтеровањем: из дефинитвне флотацијске јаловине, мешавина дефинитвне флотацијске јаловине са базалтом (10%, 20% и 40%) и мешавина дефинитвне флотацијске јаловине са туфом (20% и 40%) на различитим температурама и различитом времену, да би се нашао оптимални састав и услови кристализације за добијање применљивог материјала.*

*Резултати указују да се са повећањем, температуре (са 1100 на 1480°C) и времена синтеровања дефинитвне флотацијске јаловине (са 4 на 6h), добија стаклокерамика са већим садржајем кристала хематита (44%). Стаклокерамика од чисте дефинитвне флотацијске јаловине (синтерована на 1080°C у току 36h) испољава добре механичке особине, које се огледају у великој брзини простирања ултразвучних таласа (4500 m/s) и тврдини по Викерсу (10800 MPa), а уз то је и отпорност на термошок веома добра. Механичке особине синтетисане стаклокерамике из мешавина дефинитвне флотацијске јаловине са базалтом (1000 °C/48h) и мешавине дефинитвне флотацијске јаловине са туфом (1080°C у току 36h) су скромније. Мешавине са туфом имају знатно мању запреминску масу. Стога се дефинитвна флотацијска јаловина може примењивати као основа за добијање грађевинског материјала.*

***Кључне речи:*** *дефинитивна флотацијска јаловина, синтеровање, стакло-керамика, фазни састав, микроструктура, механичке особине.*